JOURNAL OF MATERIALS SCIENCE 28 (1993) 6575–6581

Structural features of boron nitride dense phase formation from rhombohedral modification under high static pressure

V. F. BRITUN, A. V. KURDYUMOV, I. A. PETRUSHA*
*The Institute for Materials Science Problems, and *The Institute for Superhard Materials, Ukrainian Academy of Sciences, Kiev, The Ukraine*

The real structure of boron nitride (BN) polycrystals after high-pressure treatment was investigated by X-ray and transmission electron microscopy methods. Different stages of boron nitride polycrystal evolution under high quasistatic pressure and high temperature were fixed, involving rhombohedral boron nitride twinning, one-dimensionally disordered structure, 2H, 4H, 3C dense phase formation and 3C–BN recrystallization. A new structural scheme of BN_r–BN_w transition is proposed.

1. Introduction

Structural features of boron nitride dense modification formation, namely wurtzitic (BN_w) and sphaleritic (BN_s), from hexagonal graphite-like modification, BN_g, have been studied in detail [1, 2]. Both phase-transformation mechanisms and polycrystal formation were considered, involving relaxation rearrangements following phase transition. Studies on the transformations of the second graphite-like modification, the rhombohedral one (BN_r) were begun comparatively recently [3–5]. By comparing BN_r and BN_s lattices it follows that the BN_r–BN_s transformation may take place via plane basal layer puckering with simultaneous compression along the *c*-axis. This mechanism is analogous to that of rhombohedral graphite transformation into diamond [6] and occurs without any intermediate structure formation. Here the orientation relationship between the phases should be as follows

$$[0001]\,BN_r \parallel [111]\,BN_s;\quad (001)\,BN_r \parallel (111)\,BN_s \tag{1}$$

The puckering mechanism is supposed to take place on BN_r shock compression, resulting in BN_s formation as shown elsewhere [3]. It was found [4] that under static compression of BN_r, both dense modifications are formed. BN_w formation appeared to be unexpected, because the puckering mechanism may explain only BN_s formation. BN_w under static compression was observed elsewhere [5]. Based on the textures of the starting phase and that under the transformation (001) $BN_r \parallel$ (001) BN_w, we concluded that the BN_r–BN_w transition takes place via a buckling mechanism. Earlier, this mechanism was proposed to explain graphite–lonsdaleite transformation [7] and it supposes the formation of an intermediate structure with ADAD layer sequence. The buckling mechanism results in an orientation relationship occurring between the phases

$$[0001]\,BN_r \parallel [10\bar{1}0]\,BN_w;\quad (001)\,BN_r \parallel (100)\,BN_w \tag{2}$$

No detailed study of the fine structure formed in the samples on BN_r transition into dense modifications has been carried out to date. Here, we report the results of a study of the mechanisms of real structure formation of the dense BN phase polycrystals prepared under static compression of BN_r.

2. Experimental procedure

The initial BN_r samples were pore-free plates of pyrolytic BN with 2.26 g cm^{-3} density. Quasihydrostatic compression of the samples was carried out in a toroid-type high-pressure chamber under 7.7 GPa and temperatures from 25–2600 °C. The exposure time at these temperatures was 60 s. The real structure of the samples after high-pressure treatment was studied using X-ray diffractometry (HTG-4) and transmission electron microscopy (JEM-100CX). The samples for electron microscopy were prepared by the ion-milling technique.

3. Results and discussion

3.1. BN_r initial structure

According to the X-ray and electron microscopic studies, pyrolytic BN plates possess texture {0001} and contain up to 80% rhombohedral modification (the balance is disordered BN_g). The sample's texture results from BN grain growth with basal planes (0001) orientation preferentially parallel to the substrate surface. The grain size is about 1 mm. The initial structure possesses a high defect density (10^9 cm^{-2}) confirmed by electron microscopic contrast (Fig. 1a). A weak azimuthal broadening of reflexes on selected-area diffraction (SAD) patterns corresponding to the

0022–2461

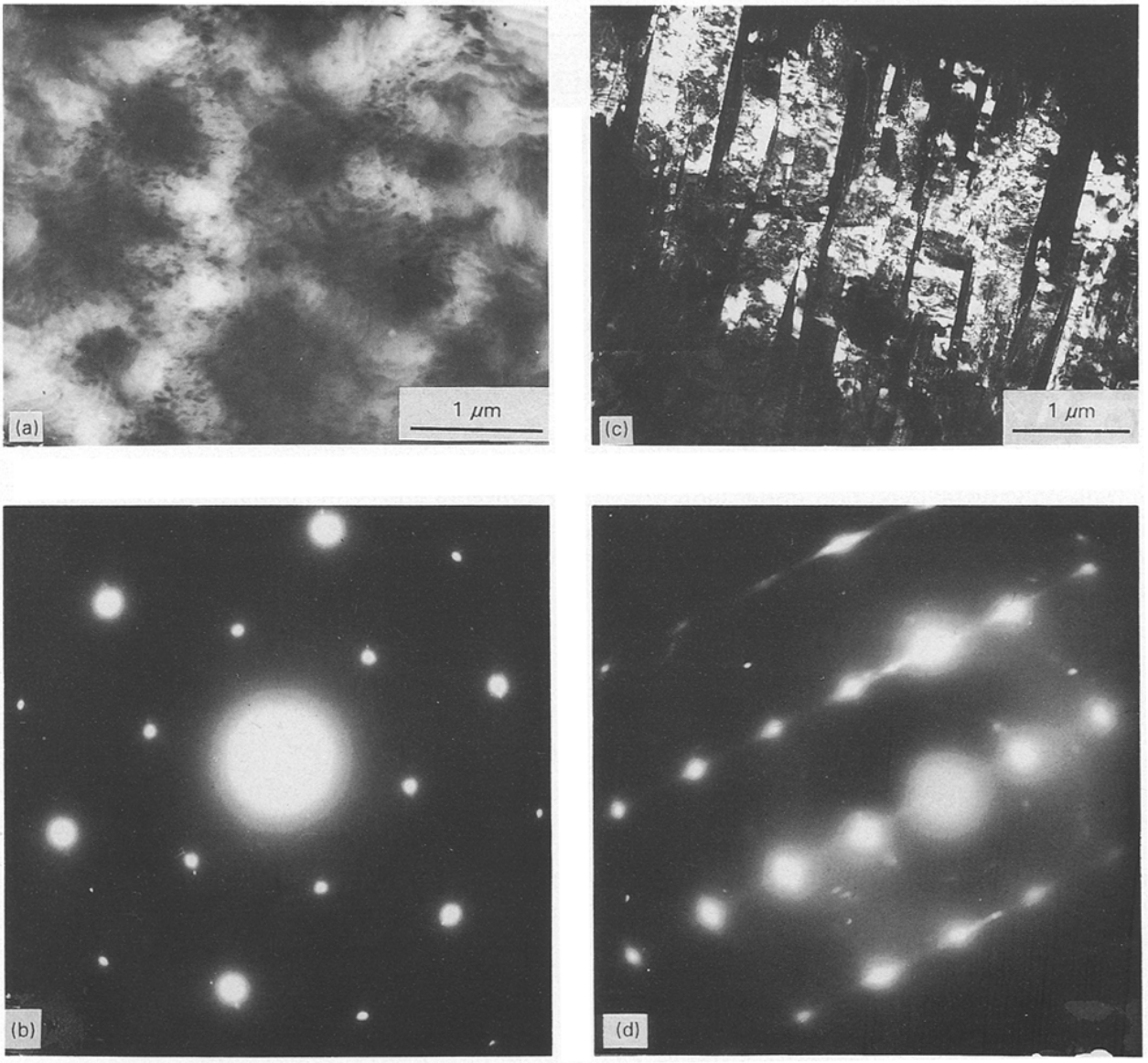

Figure 1 BN_r initial structure. (a) Transmission electron micrograph and (b) SAD pattern from the BN_r grain with the zone axis [0 0 0 1]; (c) transmission electron micrograph (dark-field image) and (d) SAD pattern from the BN_r grain with the zone axis [$\bar{2}$ 1 1 0].

basal sections (Fig. 1b) enables one to consider that dislocations are distributed randomly and do not result in grain fragmentation. On SAD patterns from prismatic sections (Fig. 1c) one can see an appreciable azimuthal broadening of reflexes, which may be related to sample lamination while preparing prismatic polished sections. Continuous diffusion streaks in the series of *O K L* reflexes can also be observed, indicating a high concentration of stacking faults (SF) in the initial BN.

3.2. Structure formed at temperatures below 1000 °C

In the samples after *P–T* treatment at 300–1000 °C the X-ray and electron microscopic studies showed BN_w dense modification (at 1000 °C transformation achieved 90%). Analysis of the diffraction patterns reveals two mechanisms of BN_w formation. Let us consider the experimental data and possible structural schemes of rearrangement during BN_r–BN_w transformation.

1. In the first case, on the SAD patterns from the two phase regions, corresponding to the [0 0 0 1]·BN_r zone axis, together with BN_r $hk0$ reflexes, those of BN_w are present. The latter result from superposition of reciprocal lattices of three equivalent cross-sections (1 2 0)*. These cross-sections are at an angle of 120° relative to each other. In fact, a ternary texture is formed in the initial single crystalline grain. (Fig. 2a and b show the SAD pattern and its index.) Analogous diffraction patterns were observed elsewhere [8] from graphite crystals partially transformed into lonsdaleite. The diffraction patterns indicate orientational relationships (2) between BN_r and BN_w. The respective mechanism of transformation should involve formation of the intermediate ADAD structure with subsequent formation of bonds with tetrahedral coordination via buckling.

Concerning intermediate structure formation in the mechanism above, it may be noted that in the two-phase samples, reflex nets were sometimes observed, which may refer to ADAD structure (reciprocal lattice cross-sections of this structure are presented elsewhere

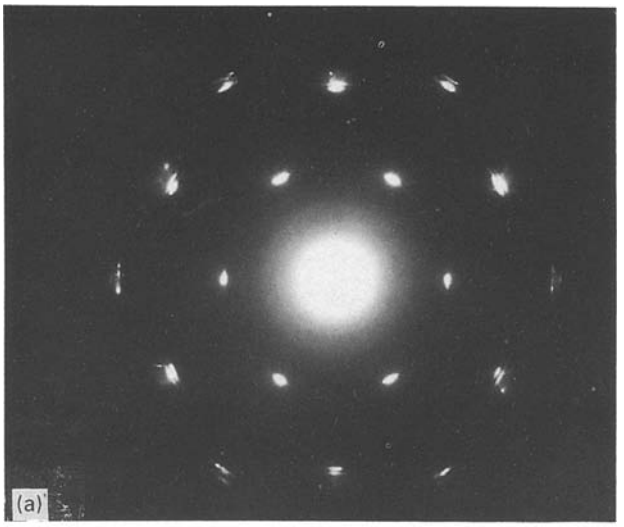

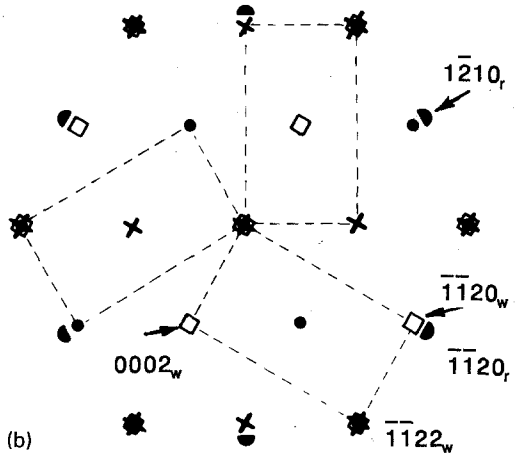

Figure 2 (a) SAD pattern and (b) index from the heterophase region (first transformation scheme). (⌣) BN_r spots, (□, ●, +) BN_w spots – different components of ternary texture.

[9]). However, this problem requires further study and we shall not dwell on it here.

2. The second mechanism is observed in the regions where phase transformation follows BN_r twinning. Twinning in BN_r was observed at a treatment temperature as low as 25 °C. The BN_r plane of the $\{1\,0\,1\}$ type was found to be that of twinning. During twinning, BN_r basal planes $(0\,0\,0\,1)$ turn around the axis of $\langle 1\,\bar{2}\,1\,0\rangle$ type by an angle of about 24°40′. Twinning in BN_r is, in fact, deformation via uniform shift along the $(1\,0\,\bar{1})$ plane with shift direction $\langle\bar{3}\,0\,3\,4\rangle$. Fig. 3 shows an electron microscopic pattern of microtwins in BN_r, the SAD pattern from the twinned section, and the twinning index.

Now let us consider the transformation mechanism in BN_r-twinned regions. SAD behaviour in these regions results from such a superposition of BN_r and BN_w reciprocal lattices that a common series of reflexes appears, i.e. the $0\,0\,L$ series of BN_w coincides with $H\,0\,L$ $(H = L)$ of BN_r. Another reflex series is arranged parallel to the common series and contains

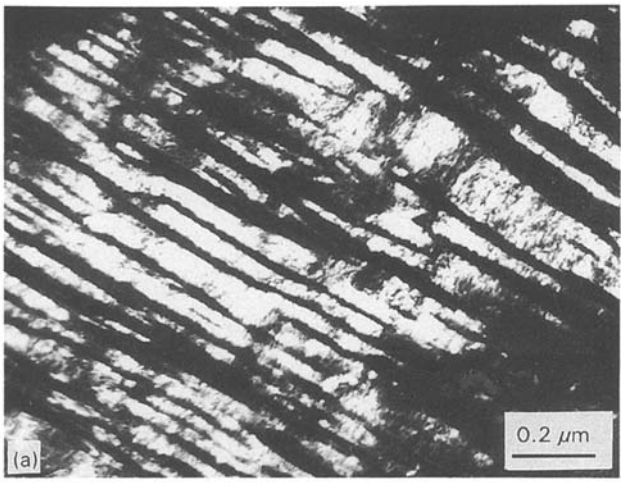

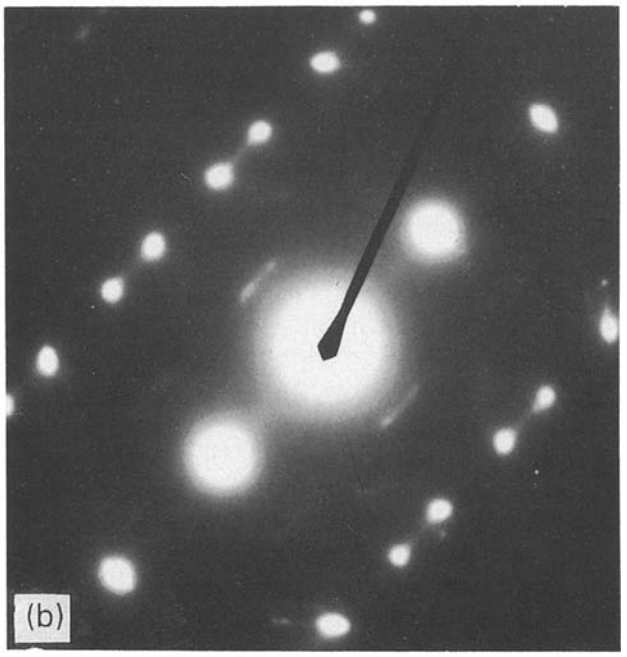

Figure 3 Twinning in BN_r. (a) Transmission electron micrograph (dark-field image) and (b) SAD pattern (zone axis $[1\,\bar{3}\,2\,1]$) from BN_r grain with twins. (c) Index of twins in BN_r.

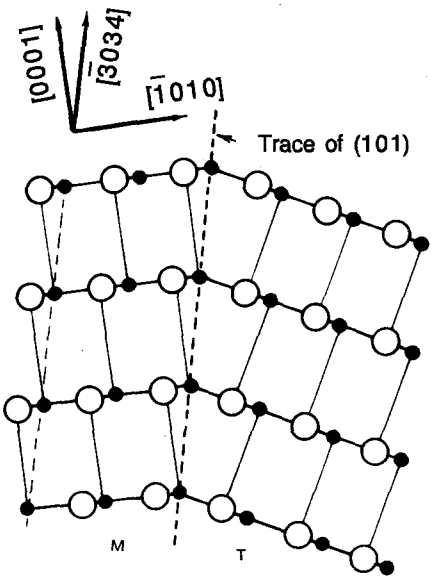

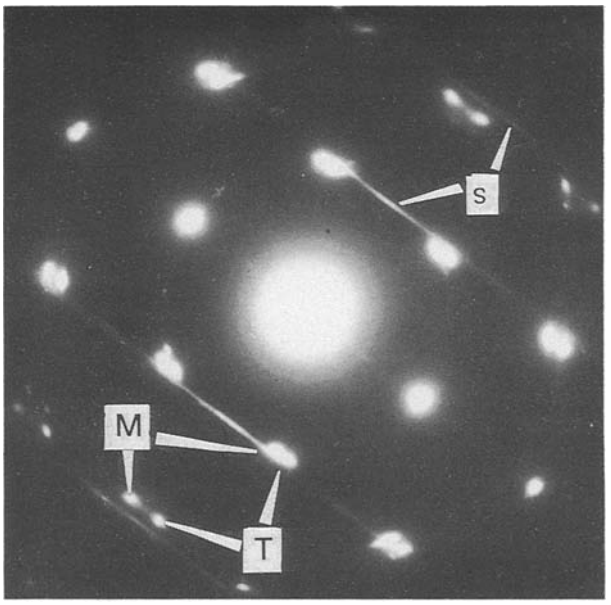

Figure 4 SAD pattern from the heterophase region (second transformation scheme). M, matrix spots of BN_r; T, twin spots of BN_r; S, streaks in $H0L$ rows of BN_w.

both matrix and twinned diffractional spots of BN_r and the $0HL$ series of BN_w reflexes with strong streaks (Fig. 4). Such reciprocal lattices superimposed unambiguously indicate the BN_w basal plane (0 0 0 1) to be formed parallel to that of BN_r twinning – (1 0 1). The axis of the BN_w zone $[1\,0\,\bar{1}\,0]$ is found to be tilted to the BN_r axis [0 0 0 1] at an angle about 12°20′ turning around the $[1\,\bar{2}\,1\,0]$ axis. Fig. 5a shows a crystallographic illustration of phase conjugation. The respective orientation relations between the phases are

$$[\bar{3}\,0\,3\,4]\ BN_r \parallel [1\,0\,\bar{1}\,0]\,BN_w;\quad (1\,0\,1)\,BN_r \parallel (0\,0\,0\,1)\,BN_w \tag{3}$$

The following hypothetical scheme of transformation resulting in the above relations (3) may be suggested. If, in some region, BN_r twinning takes place in each (1 0 1) plane, a structure is formed similar to ADAD structure (relative to the arrangement of atoms in basal planes), but different in the basal layers splitting (Fig. 5b). Such structure compression along the *c*-axis accompanied by insignificant atom shifts in (1 0 1) planes results in wurtzite structure related to the initial one via Relations 3 above. In this mechanism, twinning is a stage of dense-phase nucleation initiation. The mechanism proposed explains why in BN_r twin and matrix regions, BN_w layers of the same orientation are formed, because (1 0 1) BN_r planes preserve their orientation during twinning.

It should be noted that in the case of the second mechanism of transformation in the starting grain, a ternary texture is formed due to the neighbouring regions twinning along equivalent planes {1 0 1}.

The first or second mechanism under consideration is probably caused by BN_r grain deformation behaviour. If, in a grain, a light basal sliding is possible resulting in uniform shift with ADAD structure arising, the first transformation mechanism takes place. Under more favourable conditions for grain deformation via twinning, the second mechanism is responsible for transformation.

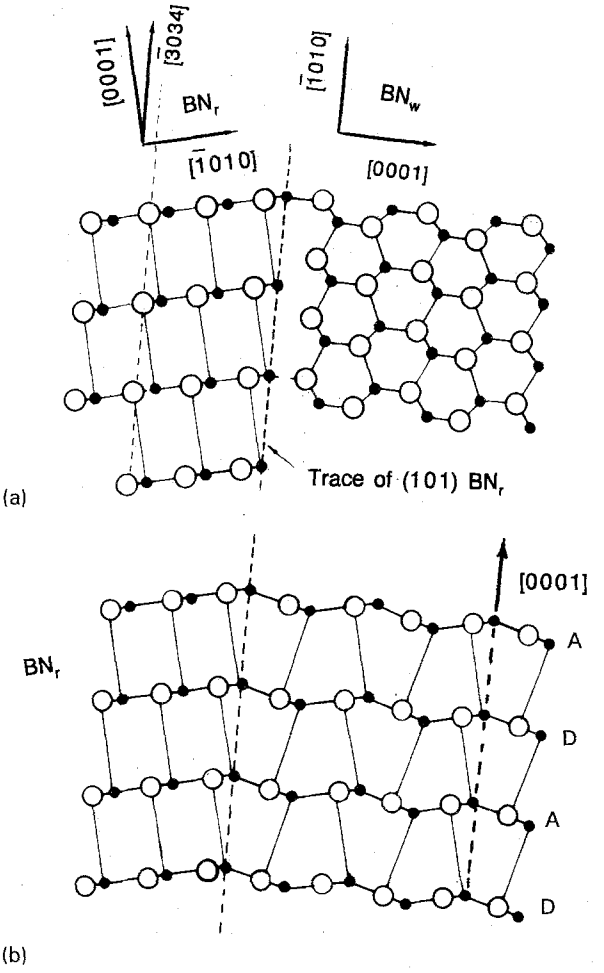

Figure 5 Crystallographic structures: (a) BN_r and BN_w phase conjugation, (b) the hypothetical intermediate structure.

3.3. Transformations at temperatures above 1000 °C

Below 1000 °C, the BN dense modification is, in fact, a one-dimensionally disordered structure (ODS) based on wurtzite phase (indicated by nearly continuous streaks in the SAD patterns and comparatively weak BN_w reflexes). On increasing the temperature up to 1300–1400 °C, the streaks are weakened and more defined BN_w reflexes appear (Fig. 6a). However, BN_w always contains a high concentration of stacking faults. At 1500–1600 °C, 4H polytype of BN was found. Fig. 6b shows SAD patterns, where reflexes of 4H structure, not coinciding with 2H structure reflexes, are indicated by arrows. The 4H polytype is found only in the mixture with wurtzite (2H) BN, no pure form was observed. 4H structure formation may be considered to be natural during transition from wurtzite (2H) to sphalerite (3C), because according to the degree of hexagonality (50%) it is the average between these structures (hexagonality degree of 2H and 3C structures is 100% and 0%, respectively).

Above 1600 °C BN_s begins to form and above 2000 °C it is the only phase present in the samples. The

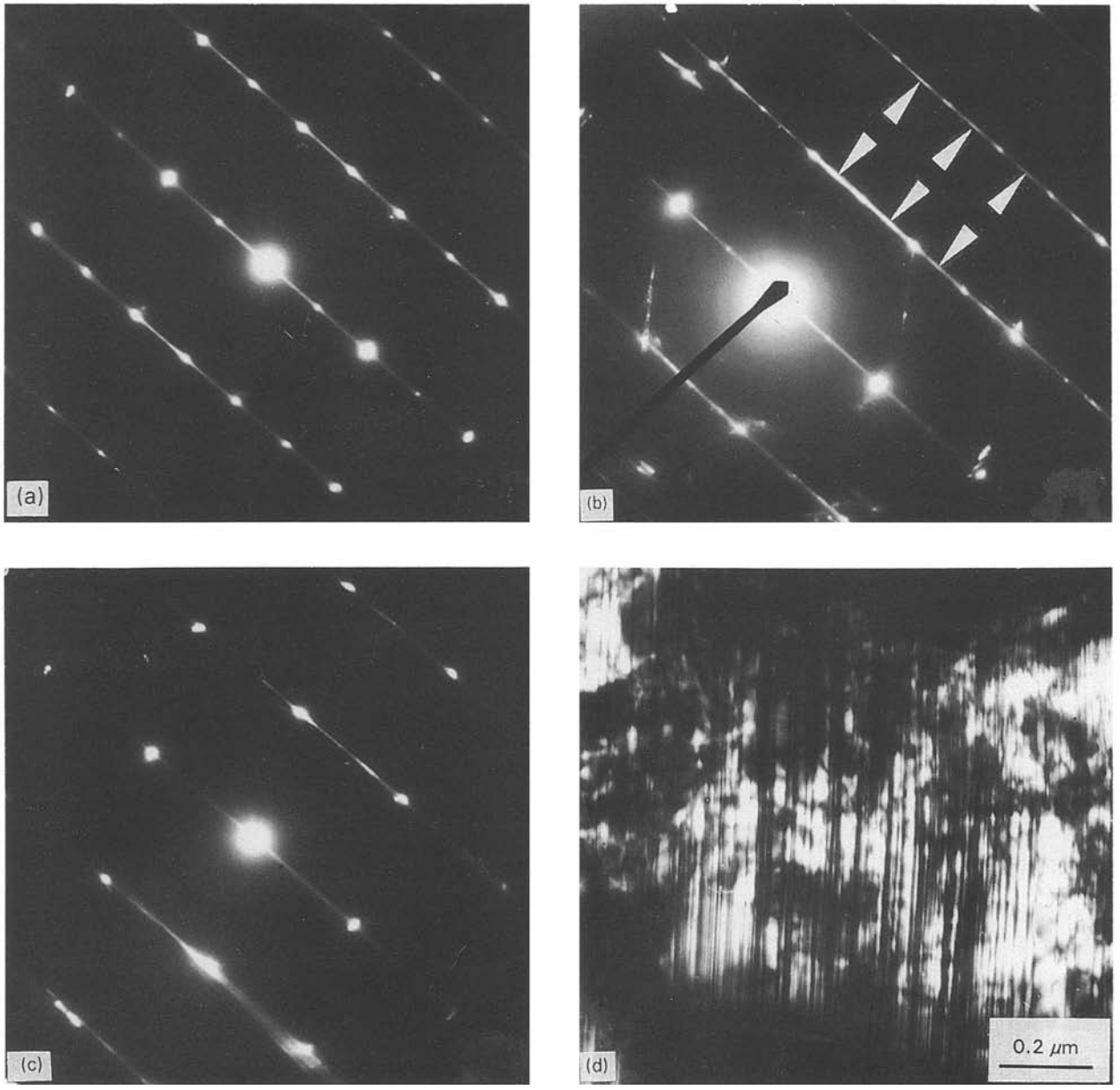

Figure 6 Transformations at temperatures above 1000 °C. SAD patterns (zone axis $[\bar{2}\,1\,1\,0]$): (a) 2H–BN, (1200 °C), (b) 2H + 4H–BN (1500 °C); (c) 3C–BN (2000 °C). (d) Transmission electron micrograph of lamellar substructure.

whole temperature range up to 2000 °C is characterized by the fact that all dense phases (ODS, 2H, 4H, 3C) are formed as grains with lamellar substructure (Fig. 6d). Such substructure results from the diffusion-free (martensitic) phase transformation BN_r–BN_w subsequently inherited during 2H–4H–3C transformations due to layer-to-layer rearrangement via ordered stacking fault formation. Under such rearrangements, the orientation relations are as follows: $[1\,0\,\bar{1}\,0]\,BN_w \parallel [1\,1\,2]\,BN_s$; $(0\,0\,0\,1)\,BN_w \parallel (1\,1\,1)\,BN_s$. The sequence of transformations observed during the high-pressure treatment temperature rise, enables one to suggest that under BN_r static loading, BN_s is formed via a stage of intermediate structure formation, i.e. ODS, 2H, 4H. The orientation relations indicate the puckering mechanism to be invalid under the given conditions.

In BN_s phase under loading at above 2000 °C, high-temperature plastic deformation begins to take place, resulting in subsequent grain fragmentation due to the appearance of subgrains and the rearrangements of lamellar substructure. The lamellar substructure vanishes completely due to BN_s primary recrystallization above 2300 °C (Fig. 7a). Primary recrystallization results in the formation of fine structure based on equiaxial grains with comparatively low intragrain defect density. Recrystallization does not destroy completely a ternary texture occurring in the initial single crystalline grain at the starting stage of transformation. In the recrystallized regions, a significant part of the BN_s grains is oriented by $(\bar{1}\,1\,2)$ planes rather close to the $(0\,0\,0\,1)$ plane of the initial BN_r, and the $\langle 1\,1\,1 \rangle$ axes of BN_s in the $(\bar{1}\,1\,2)$ planes for different grains are disoriented by an angle 120° (Fig. 7b, c).

Above 2500 °C (7.7 GPa), BN_s secondary recrystallization begins. The grain size increases up to hundreds of micrometres and the defect density does not exceed 10^{-8} cm^{-2}. The main defects in grains after secondary recrystallization are twins (Fig. 8a), similar in morphology to those of recrystallization origin in

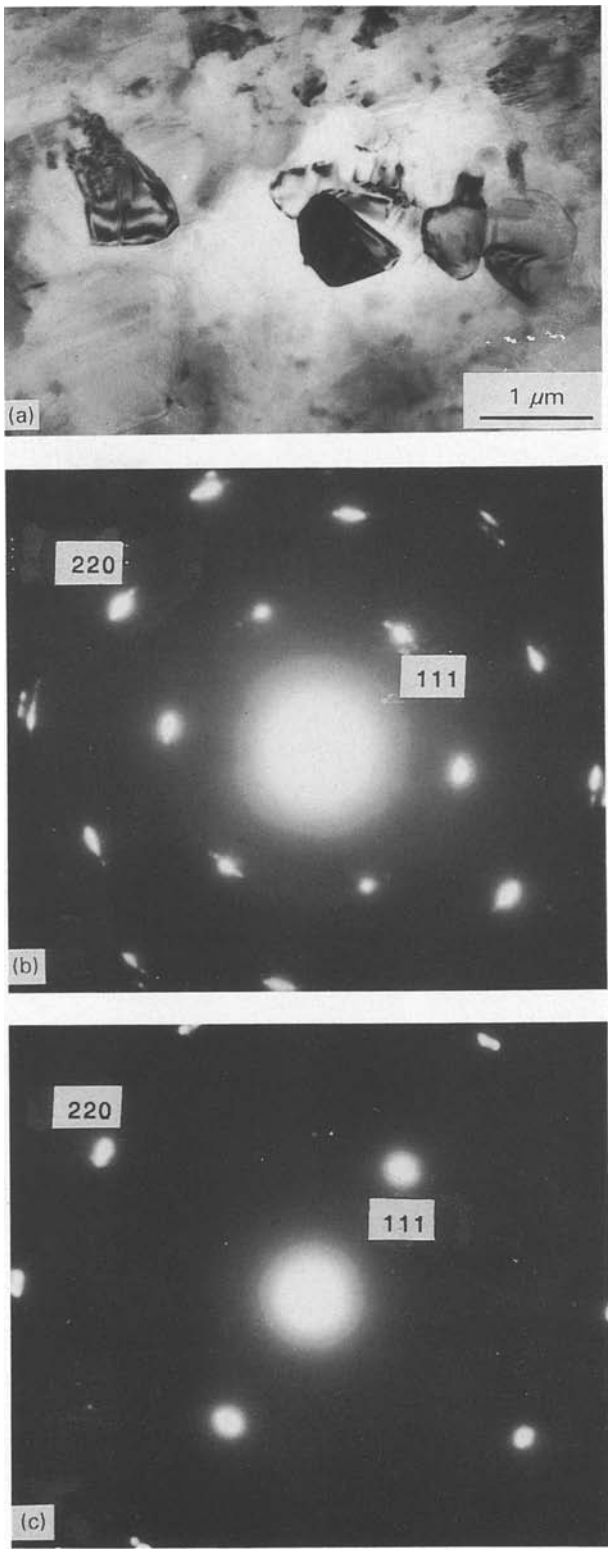

Figure 7 Primary recrystallization of BN_s. (a) Transmission electron micrograph and (b) SAD pattern from a group of grains. and (c) SAD pattern from one grain.

fcc metals [10]. In addition, local clusters of dislocations and dislocation loops are observed in grains (Fig. 8b, c). The contrast exhibited by dislocation loops (the loops themselves being in the (1 1 1) plane have strong contrast under $\bar{g} = 1\,1\,1$ and contrast from stacking faults may be observed in the loops), makes it possible to consider them Frank loops arising during point defect coagulation under conditions when their diffusion movement to the grain boundaries is hindered by a low density of dislocations and a low velocity of volume diffusion.

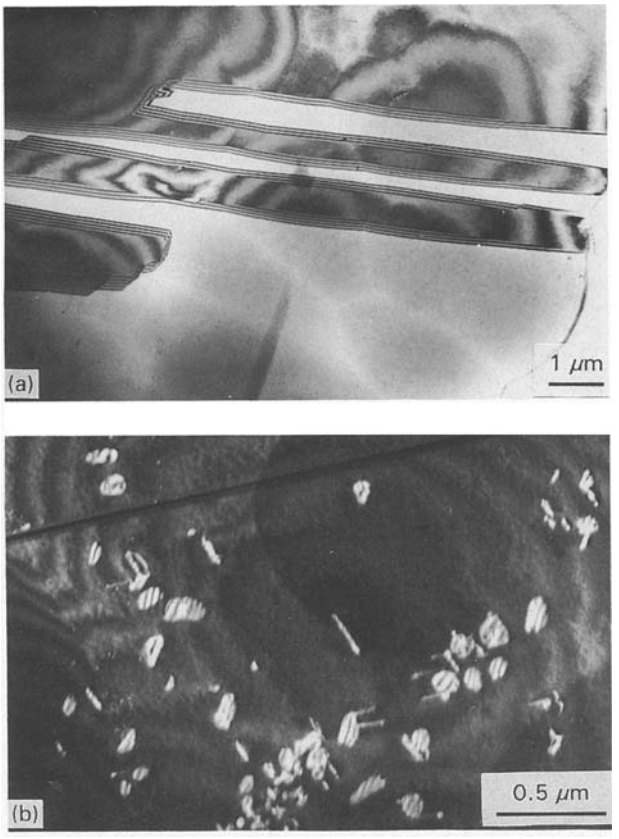

Figure 8 The substructure of BN_s grains after secondary recrystallization. (a) Twins in a BN_s grain. (b) Dislocation loops.

4. Conclusion

The studies showed rhombohedral BN under quasihydrostatic compression ($P \leqslant 7.7$ GPa) to be transformed into the wurtzite modification (below 1000 °C into a highly one-dimensionally disordered structure based on 2H–BN). BN_r–BN_w transformation may take place via two routes, the latter one related to twinning being found for the first time. Both mechanisms provide diffusion-free rearrangement and differ mainly in the method of initial structure deformation at the onset of transformation. BN_r–BN_s direct transformation via a puckering mechanism does not occur. A sphaleritic modification is formed from the wurtzite structure, due to layer-to-layer rearrangement, i.e. transformation via an intermediate structure is realized. The 4H structure of BN polytype is formed, in an average position between 2H and 3C structures, as their hexagonal form. During deformation and phase transformation of an initial single-crystalline BN grain, a ternary texture appears which is preserved throughout all subsequent stages of rearrangement up to recrystallization.

References

1. A. V. KURDYUMOV and A. N. PILYANKEVICH, "Phase transformations of carbon and boron nitride" (Naukova Dumka, Kiev, 1979) p. 188 (in Russian).

2. A. N. PILYANKEVICH and G. S. OLEYNIK, in "Vliyanie visokich davlenii na veshestvo", Vol. 1, edited by A. N. Pilyankevich, (Naukova Dumka, Kiev, 1987) p. 57 (in Russian).
3. T. SATO, T. ISHII and N. SETAKA, *J. Am. Ceram. Soc.* **65** (10) (1982) 162.
4. A. ONODERA, K. INOUE, H. YOSHIHARA, H. NAKAE, T. MATSUDA and T. HIRAI, *J. Mater. Sci.* **25** (1990) 4279.
5. I. A. PETRUSHA, A. A. SVIRID, A. H. LUCENKO, B. N. SHARUPIN and S. M. POTECHIN, "Martensitic transformation of rhombohedral boron nitride in wurtzitic–BN under high static pressure", Preprint of Institute for Superhard Materials of the Ukrainian Academy of Sciences, Kiev, 1990, p. 12 (in Russian).
6. K. LONSDALE and H. J. MILLEDGE, *Miner. Mag.* **32** (1959) 185.
7. A. V. KURDYUMOV and N. I. BORIMCHUK, *Dokl. Acad. Nauk USSR* **297** (1987) 602 (in Russian).
8. A. V. KURDYUMOV, N. F. OSTROVSKAYA and A. N. PILYANKEVICH, *Poroshkov. Metall.* **1** (1988) 34 (in Russian).
9. A. V. KURDYUMOV and G. S. OLEYNIK *Crystallogr.* **29** (1984) 792 (in Russian).
10. M. A. MEYERS and L. E. MURR, *Acta Metall.* **26** (1978) 951.

Received 1 May 1992
and accepted 5 March 1993